

Determination of the Action Spectrum of UVR-Induced Mitochondrial DNA Damage in Human Skin Cells

Jennifer A. Latimer^{1,2}, James J. Lloyd³, Brian L. Diffey¹, Paul J. Matts² and Mark A. Birch-Machin¹

Biological responses of human skin to UVR including cancer and aging are largely wavelength-dependent, as shown by the action spectra of UVR-induced erythema and nuclear DNA (nDNA) damage. A molecular dosimeter of UVR exposure is therefore required. Although mitochondrial DNA (mtDNA) damage has been shown to be a reliable and sensitive biomarker of UVR exposure in human skin, its wavelength dependency is unknown. The current study solves this problem by determining the action spectrum of UVR-induced mtDNA damage in human skin. Human neonatal dermal fibroblasts and primary human adult keratinocyte cells were irradiated with increasing doses of UVR. Dose–response curves of mtDNA damage were produced for each of the UVR sources and cell types, and an action spectrum for each cell type was determined by mathematical induction. Similarities between these mtDNA damage action spectra and previously determined nDNA damage were observed, with the most detrimental effects occurring over the shorter UVR wavelengths. Notably, a statistically significant ($P < 0.0001$) greater sensitivity to mtDNA damage was observed in dermal fibroblasts compared with keratinocytes at wavelengths > 300 nm, possibly indicating a wider picture of depth dependence in sensitivity. This finding has implications for disease/photodamage mechanisms and interventions.

Journal of Investigative Dermatology (2015) **135**, 2512–2518; doi:10.1038/jid.2015.194; published online 25 June 2015

INTRODUCTION

Most biological end points induced by exposure to UVR show a highly wavelength-specific response, often encompassing 3–4 orders of sensitivity over the spectral waveband of solar UVR (290–400 nm). These include erythema and tanning in human skin, as well as nuclear DNA (nDNA) damage and carcinogenesis (Diffey, 1991).

In addition to the nucleus, mitochondria also contain their own DNA (mitochondrial DNA (mtDNA)), linked indirectly with longevity. Both mtDNA mutations and deletions have been implicated in a number of human pathologies including cancer, and a cause-and-effect relationship between mutated/deleted mtDNA and aging has been reported in various cell types (Birch-Machin *et al.*, 1998; Schroeder *et al.*, 2008).

Skin is our main environmental interface with a significant increased risk of insult versus most other tissues.

Age-associated features including wrinkling, roughness, laxity, pigmented spots, and diffuse hyperpigmentation are most prominent in areas of the body that are most exposed to solar UVR, such as the face and hands. This suggests that the expression of these characteristics is driven primarily by exposure to solar radiation, a phenomenon known as photoaging (Berneburg *et al.*, 2004; Schroeder *et al.*, 2008). Because of the permanency of mtDNA damage, it is conceivable that exposure to UVR results in an accumulation of associated damage end points leading to an acceleration in aging, a notion that has led to the development of mtDNA as a biomarker of UVR-induced damage (using techniques developed by our group and adopted by others (Birch-Machin, 2000; Sligh *et al.*, 2002; Berneburg *et al.*, 2004)). In relation to this, several studies have found an increase in incidence of specific deletions of mtDNA in skin cancer, as well as in sun-exposed skin when compared with sun-protected skin (Birch-Machin *et al.*, 1998; Koch *et al.*, 2001; Krishnan *et al.*, 2004; Birch-Machin *et al.*, 2013). Furthermore, damage to mtDNA can be induced *in vitro* by UVR irradiation of cultured human skin cells and skin equivalents (Birch-Machin *et al.*, 1998; Birket and Birch-Machin, 2007).

Although the action spectra of UVR-induced erythema (McKinlay and Diffey, 1987) and UVR-induced nDNA damage (Setlow, 1974) have been investigated previously, UVR-induced mtDNA damage, to our knowledge, has yet to be studied. This is a significant omission as, apart from mitochondria being the source of cellular energy and major

¹Dermatological Sciences, Institute of Cellular Medicine, Newcastle University Medical School, Newcastle upon Tyne, UK; ²Procter and Gamble Greater London Innovation Centre, Surrey, UK and ³Regional Medical Physics Department, Newcastle Hospitals, Newcastle, UK

Correspondence: Mark A. Birch-Machin, Dermatological Sciences, Institute of Cellular Medicine, Newcastle University Medical School, Newcastle upon Tyne, NE2 4HH, UK. E-mail: mark.birch-machin@ncl.ac.uk

This work was performed in Newcastle upon Tyne, Tyne and Wear, UK.

Abbreviations: C(t), cycle threshold; HDfn, human dermal fibroblast neonatal; mtDNA, mitochondrial DNA; nDNA, nuclear DNA; PK, primary keratinocyte; QPCR, quantitative real-time PCR

Received 23 January 2015; revised 1 May 2015; accepted 6 May 2015; accepted article preview online 1 June 2015; published online 25 June 2015

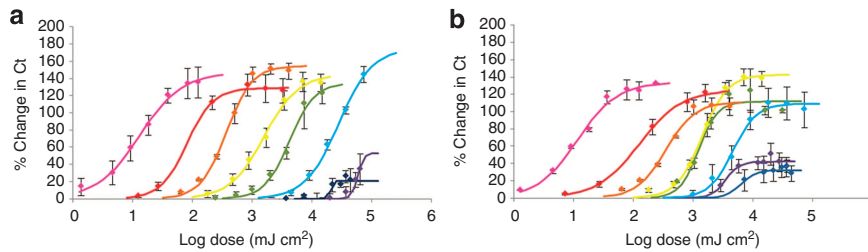


Figure 1. UVR-induced dose curves of damage. Primary keratinocyte (a) and HDFn (b) cells were irradiated with increasing doses of (from left to right) the TL12 (—), UV6 (—), TL01 (—), Helarium (—), Arimed B (—), Cleo- filter (—), and Cleo+ filter (—) UVR sources. Damage was assessed by a reduction in amplification of an 11-kb product by QPCR and is expressed as a percentage increase when compared with control (UVR protected) cells ($n \geq 3 \pm \text{SEM}$). HDFn, human dermal fibroblast neonatal.

determinant of cellular oxidative stress, mtDNA has been established as a marker of UVR exposure in skin and has a strong association with aging, as well as with skin cancer. Studying the action spectrum of UVR-induced mtDNA damage will provide important mechanistic insight into this phenomenon and may indicate new biomarkers of carcinogenesis, as well as helping guide the development of new therapeutic and behavioral approaches to modulating sun damage.

RESULTS

UVR-induced mtDNA damage

The initial damage created in mtDNA was determined by the occurrence of strand breaks / lesions within an 11-kb section of the 16.5-kb mitochondrial genome. This was quantified by the reduction in efficiency of the amplification of this product by quantitative real-time PCR (QPCR) in the damaged DNA. Damage was induced by irradiating cells with an increasing dose of UVR from UVR sources with a range of spectral output, in order to construct a dose–response damage curve.

The complete set of dose–response damage curves created by the various UVR sources in primary human adult keratinocytes (primary keratinocyte (PK)) and human dermal fibroblasts neonatal (HDFn) cells is recorded in Figure 1a and b, respectively. The dose ranges used were as follows: 0.01–3 J cm⁻² (TL12), 0.1–4 J cm⁻² (UV6), 0.1–14 J cm⁻² (TL01), 0.3–30 J cm⁻² (Helarium), 1–73 J cm⁻² (Arimed B), 4–74 J cm⁻² (Cleo- filter), and 3–37 J cm⁻² (Cleo+ filter); this equates to maximum standard erythemal dose values of 80, 50, 80, 60, 40, 10, and 2, respectively. The standard erythemal dose (Diffey *et al.*, 1997; CIE Standard, 1998) is a unit that is being introduced progressively as an erythemally weighted measure of radiant exposure equivalent to 100 J m⁻² (in contrast with the Minimum Erythema Dose, which depends upon several factors such as susceptibility to sunburn, anatomical site, time of observation, and so on). Each dose–response curve represents the mtDNA damage induced by an independent UVR source, and each data point on the curve denotes a minimum of three biologically independent experiments, each of which was analyzed three times. Each dose–response curve, therefore, comprises 72 individual data points.

An index of mtDNA damage was derived by calculating the percentage change in cycle threshold (C(t)) compared with

UVR-protected control cells. Characteristic dose effect curves could be plotted for all UVR sources in all cell types. A consistent pattern in results emerged in which curves shifted toward higher log dose values for UVR sources emitting longer wavelengths.

Action spectrum modeling

We tested the null hypothesis that the mechanism of the responses observed in Figure 1 was the same for all UVR sources (in other words, that the maximum response and slope of the dose–response curves were independent of the lamp used for irradiation). Maximum response *A* and slope parameter *c* are shown in Figure 2.

An analysis of variance test (Kruskall–Wallis) was applied to all lamp data, excluding the effect of the Cleo lamp because of differences due to issues of cell viability and also omitting a single value of *c* (0.59) from TL12 (HDFn), which appeared to be an outlier. It was concluded that there was no significant difference ($P > 0.05$) in *A* and *c* between lamps, with mean \pm SD *c* values of 0.22 ± 0.078 and 0.25 ± 0.061 for HDFn and PK, respectively. Finally, the spectral sensitivity factor *b* was examined and a significant difference ($P = 0.0015$) between lamps was found for both HDFn and PK cells.

Consequently, it was concluded that the mechanism of response was independent of UVR lamp and could, therefore, be expressed as the dose–response curve from the *i*th UVR source as follows: $Y_i = 126 / \{1 + \exp[-(x - b_i) / 0.22]\}$ and $Y_i = 157 / \{1 + \exp[-(x - b_i) / 0.25]\}$ for HDFn and PK cells, respectively. These families of curves are represented in Figure 3.

The action spectrum of UVR-induced mtDNA damage in HDFn cells (Figure 4) was derived by a process of mathematical induction. The basis of the induction approach is to estimate an action spectrum that is described by fewer parameters than the number of sources used, to calculate the logarithm of the dose expected for a given change in C(t), and to compare these calculated doses with those actually observed (Flockhart *et al.*, 2008). The optimization process, using the SOLVER facility in Excel, involves repeated adjustment of the various parameters until the closest agreement between the modeled and the observed values is achieved.

The logarithm of the observed dose (*x*) for which a change in C(t) is *A*/2 (i.e., the point of maximum slope) is given by $x = b$, with a SD Δx equal to that of the SD on *b*.

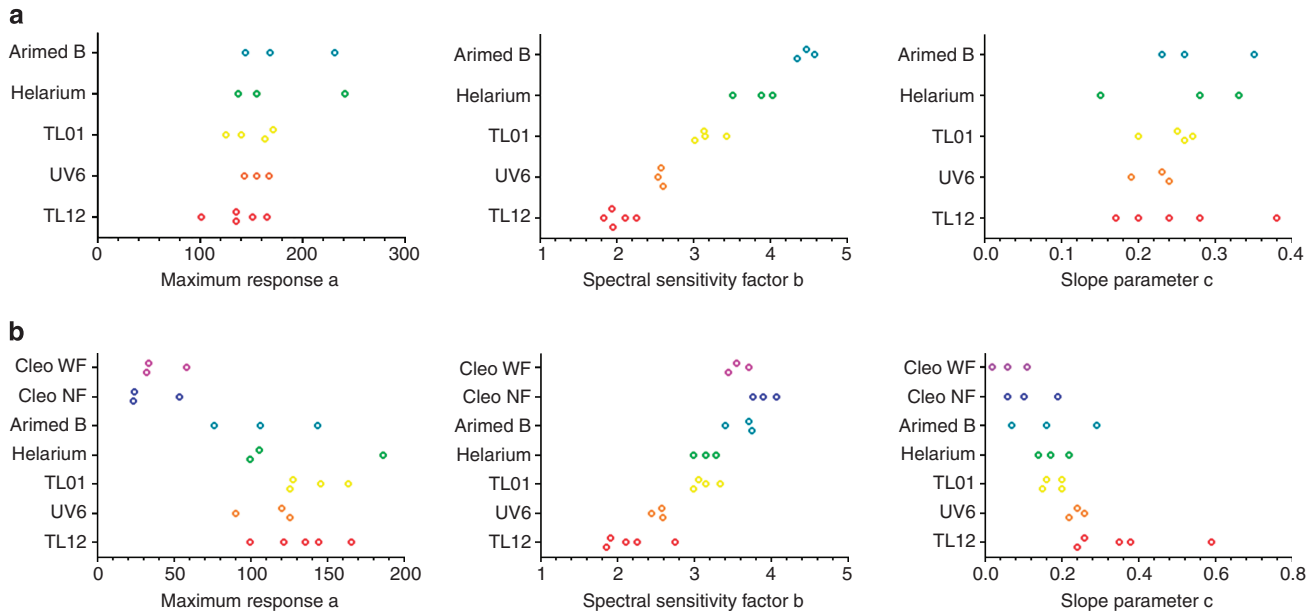


Figure 2. Differences in maximum response, spectral sensitivity, and slope of the UVR-Induced Dose Curves of Damage. Primary keratinocyte (a) and HDFn (b) Values taken from those shown in Figure 1. HDFn, human dermal fibroblast neonatal.

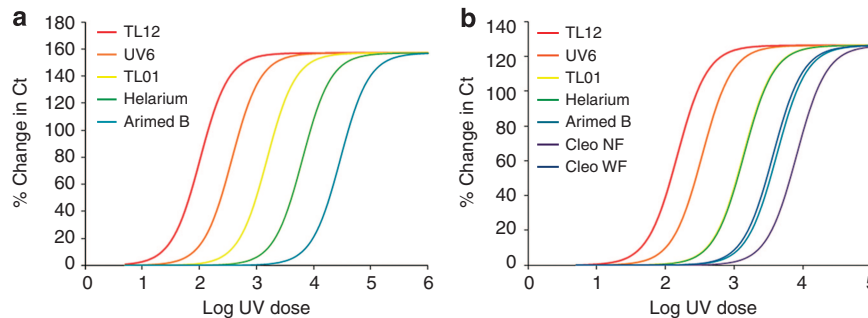


Figure 3. Normalized UVR-induced dose curves of damage. Primary keratinocyte (a) and HDFn (b) cells were irradiated with increasing doses of various UVR sources. Curves were normalized from those shown in Figure 1 by incorporating a common maximum response and slope. C(t), cycle threshold; HDFn, human dermal fibroblast neonatal.

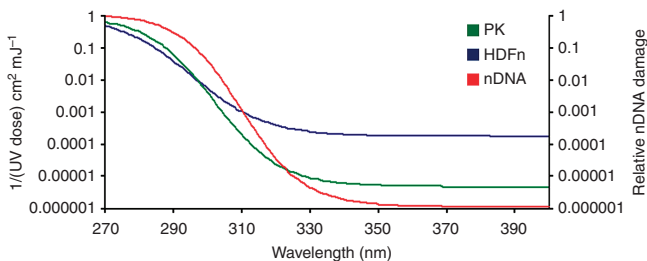


Figure 4. Action spectra of UVR-induced mitochondrial DNA (mtDNA) damage. The action spectrum for mtDNA damage in dermal fibroblasts and keratinocytes expressed as the reciprocal of the UV dose (in $\text{cm}^2 \text{mJ}^{-1}$) that results in a change in cycle threshold (C(t)) that is 50% of the plateau value (A). The action spectrum for DNA damage (Setlow, 1974) is shown in red for comparison. nDNA, nuclear DNA.

The action spectrum for DNA damage derived by Setlow (Setlow, 1974) was used as the initial candidate. This can be expressed by the following equation:

$$A(\lambda) = 1.17 \times \exp(K \times (1 / (1 + \exp((\lambda - \lambda_c) / \sigma)) - 1))$$

where $K = 13.82$, $\lambda_c = 310 \text{ nm}$, and $\sigma = 9$. The resulting action spectrum is normalized to unity at 270 nm. The optimisation process, using the SOLVER facility in Excel, involved repeated adjustment of the parameters of this spectrum until a minimum was found in the χ^2 -value, defined as follows:

$$\chi^2 = \sum_{i=1}^N (O_i - E_i)^2 / E_i$$

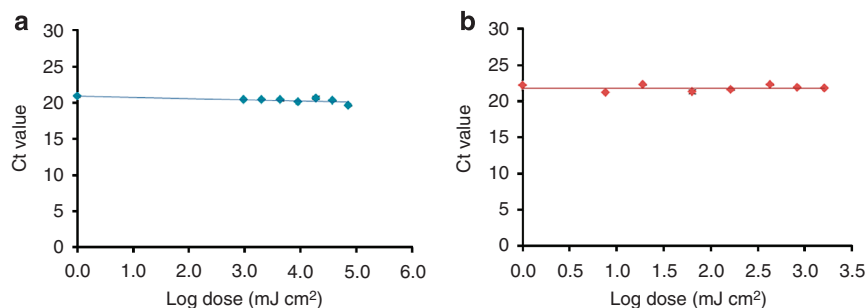


Figure 5. Determination of mitochondrial DNA (mtDNA) content following UVR exposure. Primary keratinocyte (a) and human dermal fibroblast neonatal (HDFn) (b) cells were exposed to increasing doses of the broadband UVR sources Arimed B and TL12, respectively. mtDNA content was assessed using a QPCR method to amplify an 83-bp section of mtDNA. Data expressed as the mean $n=3 \pm \text{SEM}$. Linear regression analysis of these data showed no statistically significant deviation from control ($P=0.054$ and $P=0.919$, respectively).

where O_i and E_i are the observed and expected log dose for the i^{th} lamp, respectively.

E_i is given by the expression:

$$E_i = \log \left\{ \frac{\int_{270}^{400} S(\lambda)_i / \int_{270}^{400} S(\lambda)_i \varepsilon(\lambda)}{\int_{270}^{400} S(\lambda)_i \varepsilon(\lambda)} \right\}$$

$S(\lambda)_i$ is the relative spectral irradiance of the i^{th} lamp, and $\varepsilon(\lambda)$ is the action spectrum for mtDNA damage expressed as the reciprocal of the UV dose (in $\text{cm}^2 \text{mJ}^{-1}$) that results in a change in $C(t)$ that is 50% of the plateau value (A).

Once a minimum in χ^2 was found, the probability (P_i) that the difference between E_i and O_i was statistically significant was determined as $2 \times \text{NORMSDIST}[-\text{ABS}(O_i - E_i)/\Delta x]$. The combined significance level (P) over all seven lamps is expressed as follows:

$$P = K \sum_{i=0}^6 (-\ln(K))^i / i!$$

where $K = P_1 \times P_2 \times P_3 \times P_4 \times P_5 \times P_6 \times P_7$.

This analysis resulted in the following expression for the action spectrum for UVR-induced mtDNA damage in HDFn cells:

$$\varepsilon(\lambda) = \exp(8.64 \times (1/(1 + \exp((\lambda - 295.5)/10.7)) - 1)) \text{ cm}^2 \text{ mJ}^{-1}.$$

The combined significance level (P) was calculated as 0.46 (i.e., no statistically significant difference between the cohort of observed and expected doses).

Repeating the analysis for data obtained with the PK cells resulted in an action spectrum (Figure 4) defined as follows:

$$\varepsilon(\lambda) = \exp(12.2 \times (1/(1 + \exp((\lambda - 301.9)/9.68)) - 1)) \text{ cm}^2 \text{ mJ}^{-1}.$$

The combined significance level (P) was calculated as 0.47 (i.e., no statistically significant difference between the cohort of observed and expected doses).

Overall, it is apparent that short-wavelength UVR has the greatest relative effectiveness in inducing mtDNA damage action spectra in both PK and HDFn cell types. The same is true for the action spectra reported previously for nDNA (Setlow, 1974). mtDNA was found to be more sensitive than nDNA to damage from UVR >320 nm, in both cell types.

Importantly, HDFn cells had a statistically significantly greater sensitivity to UVR >300 nm than PK cells.

DISCUSSION

Solar UVR is an environmental insult leading to photoaging and carcinogenesis in human skin. UVR covers a wide spectrum of wavelengths that have differential effects on human skin, demonstrated by the determination of a variety of action spectra, including UVR-induced erythema and nDNA damage. Over the past 15 years, mtDNA damage has been shown increasingly to be a reliable and sensitive biomarker of UVR exposure in human skin. Although mitochondria are thought to be involved in the aging process and a link between skin carcinogenesis and mitochondrial damage has been reported, the wavelength dependence of this effect has not been reported. Therefore, the aim of this study was to determine, to our knowledge, the previously unreported action spectrum for UVR-induced mtDNA damage in human skin cells.

To rule out any confounding factors, the following steps were performed. First, differences in mtDNA copy number owing to UVR exposure or different skin cell type were determined using the 83-bp assay, amplifying a short amplicon of mtDNA using QPCR. $C(t)$ values from the QPCR were then plotted and analyzed by linear regression (Figure 5). No change in mtDNA copy number was found in either PK or HDFn cells following irradiation by any of the UVR sources compared with the control, and therefore no apparent confounding effect of increasing doses of UVR were observed.

Further investigation ruled out differences in mtDNA damage because of media type or because of thermal effects of the UVR sources. For example, $C(t)$ values did not change in cells exposed to 48°C for prolonged exposures (even up to 2 hours). We also found that there was no difference in broadband UVR-induced threshold damage between the PK donors.

Clearly, in this present study, native cell types were harvested from their natural environment and compared under the same conditions as single monolayer cultures, whereas, *in situ* in living skin, these cell types have different anatomical locations within the skin compartment, i.e., basal

keratinocytes at an approximate depth of 100 μm and dermal fibroblasts located within a depth range of 100–2 mm. *In vivo*, therefore, dermal fibroblasts are exposed to only relatively small doses of shorter UVB wavelengths (<10% of incident radiation), because of Rayleigh scattering and absorption (Bruls *et al.*, 1984). It might be hypothesized, therefore, that the mtDNA of dermal fibroblasts cultured in monolayer might be more sensitive to short-wave UVR than keratinocytes, given that they are normally exposed to much lower fluxes of these wavelengths and perhaps, therefore, have not developed appropriate defense/repair mechanisms. In this study, a small difference in sensitivity was seen between the two cell types at wavelengths <300 nm. Importantly, however, differences in sensitivity to UVR-induced mtDNA damage emerged at UVR wavelengths >300 nm where a greater sensitivity was seen in fibroblasts compared with keratinocytes. Cell type-dependent response to UVR has been reported by others. D'Errico *et al.* (2007) reported that keratinocytes were more resistant than fibroblasts to the lethal effects of UVR and more efficient in the removal of cyclobutane pyrimidine dimers. Marionnet *et al.* (2010) found that there was a greater oxidative response in dermal fibroblasts in comparison with keratinocytes (demonstrated by a more rapid induction of related gene expression in these cells when irradiated with a solar simulator producing UVR approximating daily, nonzenithal sunlight, proportionally richer in UVA wavelengths). Bernerd and Asselineau (1998) have also suggested differential cell type sensitivity to UVA, supporting the opinion that dermal fibroblasts are less resistant to UVA in experiments that exposed skin equivalents to 30 J cm⁻² UVA1. One hypothesis that might explain this phenomenon is that keratinocytes contain higher levels of ferritin, involved in oxidative stress response. Ferritin provides a protective effect by chelating iron, which might otherwise catalyze the formation of damaging hydroxyl radicals induced by UVA (Qian and Van Houten, 2010). Bernerd and Asselineau (1998) hypothesized that keratinocytes could be “programmed” for stress resistance, because of their superficial location in the epidermis and resulting chronic exposure to higher doses of UVR. An example of keratinocytes being physiologically fit-for-purpose can be seen in the high concentrations of keratin protein found in these cells, providing a degree of protection against short-wave UVR because of absorption by constitutive amino acids. This notion is supported by Otto *et al.* (1999) who reported better survival rates in keratinocytes versus dermal fibroblasts after exposure to UVR.

The action spectra for UVR-induced mtDNA damage in both cell types indicated greater sensitivity to UVR wavelengths >320 nm versus nDNA (Setlow, 1974). Direct comparisons with the action spectrum for UVR-induced nDNA damage should be made with some caution, however, as that work was performed in a prokaryotic model (notably, the bacterium *Escherichia coli*). Nonetheless, aside from anatomical differences such as the presence / absence of a nuclear membrane, the inferred relatively greater sensitivity of mtDNA versus nDNA to UVR damage may be because of the close proximity of mtDNA to the intra-mitochondrial electron transport chain. Reactive oxygen species generated by longer

UVR wavelengths would be incremental to the significant source of reactive oxygen species already generated by the electron transport chain.

Furthermore, it has been reported previously that there is an increase in nucleotide excision repair, a major DNA repair pathway, in keratinocytes exposed to low-dose UVB (Maeda *et al.*, 2001). When compared with nDNA, the repair of mtDNA is significantly more limited because of a lack of nucleotide excision repair (Birch-Machin *et al.*, 2013), and therefore the apparent relative difference in mtDNA and nDNA damage may also be partly because of differing repair mechanisms/efficiency. In addition to limited repair mechanisms, mtDNA is also more vulnerable to damage, as it lacks histones that are associated with nDNA protection (Birch-Machin *et al.*, 2013).

There is an established link between reactive oxygen species production, mtDNA damage, and skin aging (Anderson *et al.*, 2014). These new data clearly support the continued need for systems to manage sun exposure (including appropriate clothing, behavior, and sunscreens). Furthermore, it is not unreasonable to hypothesize that topical supplementation with antioxidant species designed specifically to reduce mtDNA damage from oxidative stress may yet prove to have a useful role in the prevention and management of skin aging. This is especially important given that there is increasing evidence of a link between mtDNA dysfunction and a spectrum of deleterious skin manifestations (Boulton *et al.*, 2014).

This study has confirmed, as seen with the action spectra of UVR-induced erythema and nDNA damage, that the shorter UVR wavelengths are the most detrimental to human skin. Importantly, our analysis found that there was a statistically significant ($P < 0.0001$) greater sensitivity to UVR-induced mtDNA damage observed in human dermal fibroblasts compared with human keratinocyte cells. This finding has important implications for disease and photodamage mechanisms and interventions, as it may indicate a depth dependence in sensitivity to UVR-induced mtDNA damage in human skin.

MATERIALS AND METHODS

Cell culture

Human neonatal dermal fibroblast cells, HDFn (Invitrogen, Life Technologies, Paisley, UK), were maintained in DMEM (Lonza, Slough, UK) containing 10 % fetal calf serum (Lonza), 5 IU ml⁻¹ Penicillin, and 5 g ml⁻¹ streptomycin (Lonza), at 37 °C with 5% CO₂. Human keratinocyte cells were obtained from 15 adult male patient samples (aged 24–74 years) from the Royal Victoria Infirmary, Newcastle. Ethics approval was granted for this work by the Newcastle and North Tyneside Research Ethics Committee (Ref 08/H0906/95), and the research use of the samples was in accordance with the terms of the written informed consent. Cells were maintained in EpiLife medium (Gibco, UK) supplemented with 0.2% Human Keratinocyte Growth Supplement (HKGS; Gibco, Life Technologies, Paisley, UK), 5 IU ml⁻¹.

Penicillin, and 5 g ml⁻¹ streptomycin (Lonza) at 37 °C with 5% CO₂.

Irradiation method

Cells were irradiated in 60-mm dishes when they had been grown to confluent monolayers. Before irradiation, the medium was removed

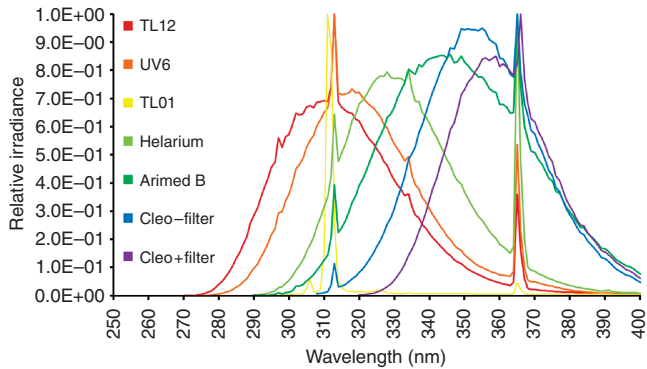


Figure 6. Spectral Chart. This figure shows the spectral output of the different UVR lamps used in the study.

and cells were washed with phosphate-buffered saline. Either phenol red-free DMEM minus fetal calf serum (HDFns) or phosphate-buffered saline (PK) was then added and the lids of the dishes were removed. For the mock control, cells were covered in aluminum foil and placed under the lamps for the same duration as the irradiated cells. For PK experiments, a minimum of three different donors were used per irradiation source. The cells were irradiated with various UVR sources, as shown in Figure 6 and as follows: TL01 (Philips TL 20W/01 RS; 22% UVA), TL12 (Philips TL 20W/12 RS; 48% UVA), UV6 (Waldmann F85/100W-UV6; 63% UVA), Helarium (Helarium R1.01, Osram, Munich, Germany; 88% UVA), Arimed B (Wolff System Helarium B1-12-40W/BPIN, Wolff System, Kennesaw, Germany; 96% UVA), and Cleo (Cleo performance 100W-R, IsoLde, Stuttgart, Germany; 99.3%; 100% UVA when used with a glass filter). To induce the required threshold damage, irradiation times varied from 0.5 to 30 minutes. Immediately following UVR treatment, the medium was removed and the cells were washed with phosphate-buffered saline before further analysis.

Quantification of mtDNA damage

For damage assessment, DNA was extracted using a QIAamp DNA mini kit as per the manufacturer's instructions (Qiagen, Manchester, UK). The content of mtDNA was determined by amplification of an 83-bp fragment of the 16.5-kb mitochondrial genome by QPCR, as shown previously (Koch *et al.*, 2001; Oyewole *et al.*, 2014), and no difference between samples was found. Damage within mtDNA was established by amplification of a 11-kb segment of the 16.5-kb mitochondrial genome by QPCR, as previously described (Passos *et al.*, 2007; Oyewole *et al.*, 2014).

Analysis of mtDNA damage

The number of cycles of PCR required to amplify a consistent amount of the 11-kb product was measured by fluorescence, and it is known as the $C(t)$. The change in the $C(t)$ value in samples exposed to a range of doses of the various UVR sources with differing spectral emissions was expressed relative to un-irradiated controls. These changes in $C(t)$ were assumed to be related to UVR dose by a sigmoid curve of the form:

$$Y = A / \{1 + \exp[-(x - b)/c]\}$$

where x is the logarithm to the base 10 of the UV dose at which the change in $C(t)$ is Y , A is the maximum response corresponding to the

maximum damage created by each UVR source, b is a parameter relating to the spectral sensitivity of a particular UV source in initiating the effect (i.e., aligned to the action spectrum of UVR induced mtDNA damage), and c is related to the maximum slope of the dose response curve by the expression $c = A / (4 \times \text{maximum slope})$.

CONFLICT OF INTEREST

The authors state no conflict of interest.

ACKNOWLEDGMENTS

This work was supported by the Engineering and Physical Sciences Research Council (EPSRC; EPSRC CASE award with Procter and Gamble).

REFERENCES

- Anderson A, Bowman A, Boulton S *et al.* (2014) A role for human mitochondrial complex II in the production of reactive oxygen species in human skin. *Redox Biol* 2:1016–22
- Berneburg M, Plettenberg H, Medve-Konig K *et al.* (2004) Induction of the photoaging-associated mitochondrial common deletion *in vivo* in normal human skin. *J Invest Dermatol* 122:1277–83
- Bernerd F, Asselineau D (1998) UVA exposure of human skin reconstructed *in vitro* induces apoptosis of dermal fibroblasts: subsequent connective tissue repair and implications in photoaging. *Cell Death Differ* 5:792–802
- Birch-Machin MA (2000) Mitochondria and skin disease. *Clin Exp Dermatol* 25: 141–6
- Birch-Machin MA, Russell EV, Latimer JA (2013) Mitochondrial DNA damage as a biomarker for ultraviolet radiation exposure and oxidative stress. *Br J Dermatol* 169(Suppl 2):9–14
- Birch-Machin MA, Tindall M, Turner R *et al.* (1998) Mitochondrial DNA deletions in human skin reflect photo rather than chronologic aging. *J Invest Dermatol* 110:149–52
- Birket MJ, Birch-Machin MA (2007) Ultraviolet radiation exposure accelerates the accumulation of the aging-dependent T414G mitochondrial DNA mutation in human skin. *Aging Cell* 6:557–64
- Boulton SJ, Bowman A, Koohgoli R *et al.* (2014) Skin manifestations of mitochondrial dysfunction: more important than previously thought. *Exp Dermatol* 24:12–3
- Bruls WA, Slaper H, van der Leun JC *et al.* (1984) Transmission of human epidermis and stratum corneum as a function of thickness in the ultraviolet and visible wavelengths. *Photochem Photobiol* 40:485–94
- CIE Standard (1998) *Erythema Reference Action Spectrum an Standard Erythema Dose*. CIE S 007/E-1998 Commission Internationale de l'Éclairage: Vienna
- D'Errico M, Lemma T, Calcagnile A *et al.* (2007) Cell type and DNA damage specific response of human skin cells to environmental agents. *Mutat Res* 614:37–47
- Diffey BL (1991) Solar ultraviolet radiation effects on biological systems. *Phys Med Biol* 36:299–328
- Diffey BL, Jansen CT, Urbach F *et al.* (1997) The standard erythema dose: a new photobiological concept. *Photodermatol Photoimmunol Photomed* 13: 64–6
- Flockhart RJ, Diffey BL, Farr PM *et al.* (2008) NFAT regulates induction of COX-2 and apoptosis of keratinocytes in response to ultraviolet radiation exposure. *FASEB J* 22:4218–27
- Koch H, Wittern KP, Bergemann J (2001) In human keratinocytes the Common Deletion reflects donor variabilities rather than chronologic aging and can be induced by ultraviolet A irradiation. *J Invest Dermatol* 117:892–7
- Krishnan KJ, Harbottle A, Birch-Machin MA (2004) The use of a 3895 bp mitochondrial DNA deletion as a marker for sunlight exposure in human skin. *J Invest Dermatol* 123:1020–4
- Maeda T, Chua PP, Chong MT *et al.* (2001) Nucleotide excision repair genes are upregulated by low-dose artificial ultraviolet B: evidence of a photo-protective SOS response? *J Invest Dermatol* 117:1490–7

- Marionnet C, Pierrard C, Lejeune F *et al.* (2010) Different oxidative stress response in keratinocytes and fibroblasts of reconstructed skin exposed to non extreme daily-ultraviolet radiation. *PLoS One* 5: e12059
- McKinlay AF, Diffey BL (1987) A reference action spectrum for ultraviolet induced erythema in human skin. *CIE J* 6:17–22
- Otto AI, Riou L, Marionnet C *et al.* (1999) Differential behaviors toward ultraviolet A and B radiation of fibroblasts and keratinocytes from normal and DNA-repair-deficient patients. *Cancer Res* 59:1212–8
- Oyewole AO, Wilmot MC, Fowler M *et al.* (2014) Comparing the effects of mitochondrial targeted and localized antioxidants with cellular antioxidants in human skin cells exposed to UVA and hydrogen peroxide. *FASEB J* 28:485–94
- Passos JF, Saretzki G, Ahmed S *et al.* (2007) Mitochondrial dysfunction accounts for the stochastic heterogeneity in telomere-dependent senescence. *PLoS Biol* 5:e110
- Qian W, Van Houten B (2010) Alterations in bioenergetics due to changes in mitochondrial DNA copy number. *Methods* 51:452–7
- Schroeder P, Gremmel T, Berneburg M *et al.* (2008) Partial depletion of mitochondrial DNA from human skin fibroblasts induces a gene expression profile reminiscent of photoaged skin. *J Invest Dermatol* 128: 2297–303
- Setlow RB (1974) Wavelengths in sunlight effective in producing skin cancer—theoretical analysis. *Procee Natl Acad Sci USA* 71:3363–6
- Sligh JE, Eshaghian A, Musiek AC *et al.* (2002) Mitochondrial DNA in aging skin and in nonmelanoma skin cancer. *J Invest Dermatol* 119:101